Acta Crystallographica Section F
Structural Biology and Crystallization Communications
ISSN 1744-3091

Expression, purification and preliminary X-ray analysis of the *Neisseria meningitidis* outer membrane protein PorB

Mikio Tanabe[a]‡ and Tina M. Iverson[a,b]*

[a]Department of Pharmacology, Vanderbilt University Medical Center, Nashville, TN 37232-6600, USA, and [b]Department of Biochemistry, Vanderbilt University Medical Center, Nashville, TN 37232-6600, USA

‡ Present address: Martin Luther University Halle-Wittenberg, Institut für Biochemie und Biotechnologie, 06120, Halle (Salle), Germany.

Correspondence e-mail: tina.iverson@vanderbilt.edu

Received 5 June 2009
Accepted 14 August 2009

The *Neisseria meningitidis* outer membrane protein PorB was expressed in *Escherichia coli* and purified from inclusion bodies by denaturation in urea followed by refolding in buffered LDAO on a size-exclusion column. PorB has been crystallized in three different crystal forms: *C*222, *R*32 and $P6_3$. The *C*222 crystal form may contain either one or two PorB monomers in the asymmetric unit, while both the *R*32 and $P6_3$ crystal forms contained one PorB monomer in the asymmetric unit. Of the three, the $P6_3$ crystal form had the best diffraction quality, yielding data extending to 2.3 Å resolution.

1. Introduction

The Gram-negative bacterium *Neisseria meningitidis* is a major causative agent of bacterial meningitis, an infection hallmarked by inflammation of the protective membranes of the brain and spinal cord (Stephens *et al.*, 2007). Six serogroups of *N. meningitidis* (A, B, C, X, Y and W135) are responsible for most life-threatening meningococcal meningitis disease and account for worldwide morbidity and at least 10 000 deaths annually. Although several vaccines are currently available for *N. meningitidis*, none are effective for serogroup B, which causes more than 50% of infections in industrialized countries (Girard *et al.*, 2006).

The *N. meningitidis* outer membrane protein (OMP) PorB is a pore-forming β-barrel protein that is essential for the survival of the organism. PorB contributes to neisserial infection through multiple unusual mechanisms (Massari *et al.*, 2003). Firstly, PorB spontaneously transfers from *N. meningitidis* and inserts into the host mitochondrial outer membrane. In the mitochondrion, PorB may interact with the mitochondrial voltage-dependent anion channel (Massari *et al.*, 2000; Müller *et al.*, 2002), which is likely to influence the mitochondrial membrane potential and cellular apoptosis (Müller *et al.*, 1999; Massari *et al.*, 2000). Furthermore, ATP and GTP may regulate the selectivity and gating of PorB in the mitochondrial membrane (Rudel *et al.*, 1996), which may contribute to host accommodation of this channel.

The location of PorB in the bacterial outer membrane allows PorB to be recognized by the immune system (Singleton *et al.*, 2005; Massari *et al.*, 2006). This makes *N. meningitidis* PorB an attractive target for vaccine development. As a result, both purified PorB and outer membrane vesicles containing PorB are currently being used to develop new vaccines against *N. meningitidis* (Girard *et al.*, 2006; Nøkleby *et al.*, 2007). Purified recombinant PorB induces an immune response in mouse models, which suggests that a protein-based vaccine could be efficacious (Wright *et al.*, 2002).

Biochemical and spectroscopic characterization of PorB have demonstrated that PorB is composed of 30–40% β-strands and is likely to form a 16-stranded trimeric porin (van der Ley *et al.*, 1991; Minetti *et al.*, 1997; Derrick *et al.*, 1999). A topology model suggests that the pore is regulated by long inter-strand loops that gate transmembrane solute translocation (van der Ley *et al.*, 1991; Derrick *et al.*, 1999). This architecture for regulation of gating is distinct from the

large folded C-terminal plug domain that hallmarks OMP transporters (Moeck & Coulton, 1998; Wiener, 2005). Here, we report the crystallization and X-ray diffraction analysis of PorB from *N. meningitidis*.

2. Material and methods

2.1. Cloning and expression

The gene encoding PorB was amplified from a clinical isolate of *N. meningitidis* (Kilic *et al.*, 2006; a generous gift from Dr YiWei Tang, Department of Infectious Disease, Vanderbilt University Medical Center) using the previously described sense (5′-GGG GTA GAT CTG CAG GTT ACC TTG TAC GGT ACA ATT AAA GCA GGC GT) and antisense (5′-GGG GGG GTG ACC CTC GAG TTA GAA TTT GTG ACG CAG ACC AAC) primers (Feavers *et al.*, 1992). The PCR-amplified fragment was digested with *Bgl*II/*Xho*I and then cloned into the *Bam*HI/*Xho*I sites of the pET21b expression vector without any affinity tags. Recombinant PorB expression was performed using modified *Escherichia coli* BL21 (DE3) cells (Locher & Rosenbusch, 1997). Cells were grown in LB medium at 303 K with 100 µg ml^{-1} ampicillin until an OD_{600} of 0.5 was reached. PorB expression was induced by the addition of isopropyl β-D-1-thio-galactopyranoside (IPTG) to a final concentration of 0.3 m*M*. The cells were incubated with shaking for 4 h at 310 K and then harvested by centrifugation at 5000*g* for 20 min at 277 K. Using this protocol, PorB was expressed into inclusion bodies (Qi *et al.*, 1994). Cells expressing seleno-L-methionine-incorporated PorB were grown in minimal medium supplemented with 25 mg l^{-1} seleno-L-methionine (SeMet) by inhibition of the methionine-biosynthesis pathway (van Duyne *et al.*, 1993).

2.2. Protein purification

Purification of *N. meningitidis* PorB was modified from a previously described protocol (Qi *et al.*, 1994; Tanabe & Iverson, 2009). Cell pellets were resuspended in breaking buffer (10 m*M* Tris–HCl, 5 m*M* EDTA pH 8.0) supplemented with 1 µg ml^{-1} DNaseI and 0.5 m*M* phenylmethylsulfonyl fluoride (PMSF) and were lysed by sonication on ice (60 Sonic Dismembrator, Fisher Scientific). The insoluble material was isolated by centrifugation at 30 000*g* for 30 min in an SS-34 rotor (Sorvall). The pellet was resuspended in TSE buffer (20 m*M* Tris–HCl pH 7.5, 200 m*M* NaCl, 1 m*M* EDTA) supplemented with 2% Triton X-100. The suspension was stirred for 1 h and insoluble material was sedimented by centrifugation at 30 000*g* for 20 min. The pellet was washed three times with TSE buffer supplemented with 2% Triton X-100 and then with TSE buffer alone in order to remove the detergent.

Approximately 1 g of inclusion bodies (from 400 ml LB culture) was resuspended in 1 ml denaturing buffer (50 m*M* Tris–HCl pH 7.5, 200 m*M* NaCl, 7.2 *M* urea) and sonicated for 1 min in a bath sonicator; it was then quickly diluted with 2 ml detergent buffer [50 m*M* Tris–HCl pH 7.5, 200 m*M* NaCl, 10% lauryldimethylamine *N*-oxide (LDAO)] and sonicated for 1 min in a bath sonicator. After 10 min incubation, the insoluble material was sedimented by centrifugation at 20 000*g* for 20 min. The clarified soluble material was passed through a 0.22 µm filter and loaded onto a Hi-Load Superdex 200 16/60 size-exclusion column equilibrated with TSE buffer supplemented with 0.15% LDAO. The elution time was consistent with a trimer (Fig. 1*a*). For SeMet PorB, all buffers were supplemented with 5 m*M* 2-mercaptoethanol.

Prior to crystallization, the purified protein was concentrated to 15 mg ml^{-1} in crystallization setup (CS) buffer (20 m*M* Tris–HCl pH 7.5, 200 m*M* NaCl) supplemented with one of several types of zwitterionic detergents [0.1% LDAO, 0.01% tetradecyl-*N*,*N*′-dimethylglycine (TDDG), 0.02% Fos-choline 14, 0.002% Fos-choline 16, 0.2% LAPAO (3-laurylamido-*N*,*N*′-dimethylpropyl aminoxide), 0.3% Anzergent 3-12 or 0.03% Anzergent 3-14]. The sample purity was assessed by SDS–PAGE of protein samples suspended in SDS sample buffer (50 m*M* Tris–HCl pH 6.8, 2% SDS, 5% glycerol, 1% 2-mercaptoethanol and 0.004% bromophenol blue) without heat

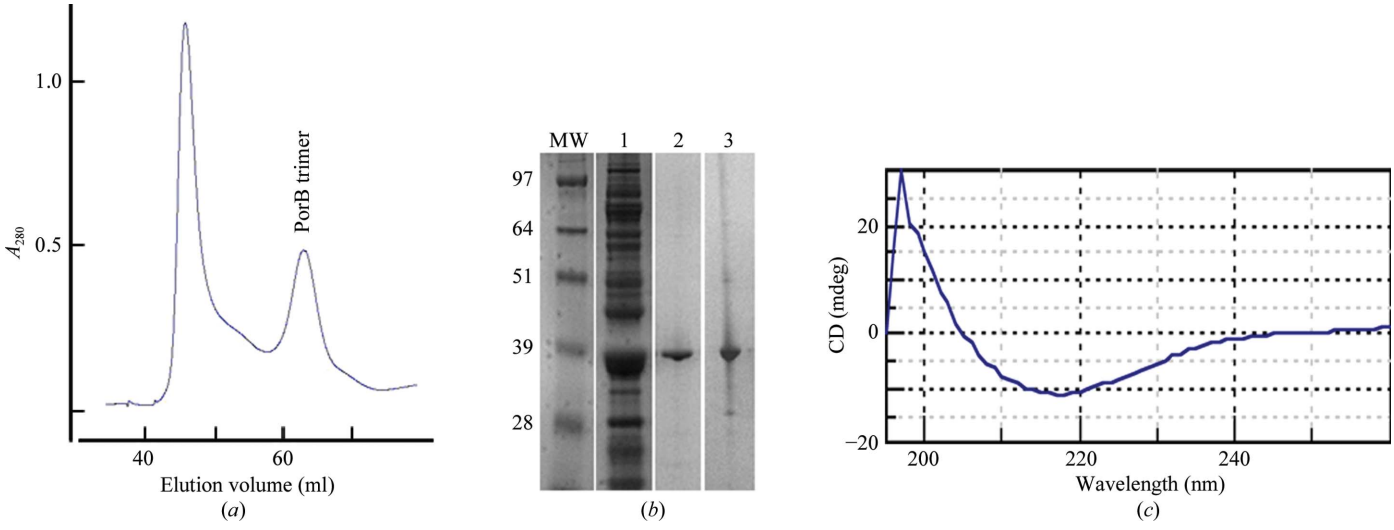

Figure 1
Purification of *N. meningitidis* PorB. (*a*) Size-exclusion chromatogram of PorB on a Hi-Load Superdex 200 16/60 size-exclusion column (120 ml bed volume) following refolding from inclusion bodies. Two peaks are observed. The first peak elutes at the void volume (45 ml) and is likely to be protein that was not correctly refolded. The second peak (64 ml) is consistent with an approximate molecular weight of 150 kDa. Since the molecular weight of a PorB monomer is 38 kDa and the detergent micelle is likely to increase the apparent molecular mass on size exclusion, this suggests that PorB refolded from inclusion bodies forms the physiologically relevant trimer. (*b*) SDS–PAGE analysis of PorB during purification from inclusion bodies. Lane 1 shows whole cell lysate. Lane 2 shows PorB purified from the inclusion bodies following size-exclusion chromatography. Lane 3 shows protein crystals of PorB in space group $P6_3$ dissolved in the purification buffer. The protein from the dissolved crystals was independently confirmed as PorB by mass-spectrometric analysis. (*c*) Far-UV CD spectrum of *N. meningitidis* PorB. The negative band at 218 nm and positive band at 196 nm are typical of a β-barrel structure.

treatment (Fig. 1*b*). The identity of PorB was independently confirmed by protein excision, in-gel digestion with trypsin protease and subsequent MALDI–TOF/TOF and ESI–LC/MS/MS mass spectrometry at the Vanderbilt University Proteomics core facility, giving a combined coverage of 89.5% of the predicted protein sequence. The β-sheet percentage of PorB at 0.7 mg ml^{-1} was confirmed by circular-dichroism (CD) spectroscopy (Fig. 1*c*) at 298 K using a Jasco J-810 CD spectropolarimeter. The solution was in a 1 mm path-length cell and the spectra were recorded with 20 nm min^{-1} scanning time. The protein concentration was estimated using the BCA protein assay (Pierce).

2.3. Crystallization

Initial sparse-matrix crystallization screening of 15 mg ml^{-1} PorB sampled 1440 chemically distinct crystallization conditions using a Mosquito crystallization robot (TTP LabTech). Both sitting and hanging drops comprised of 200 nl protein solution plus 200 nl reservoir solution were equilibrated against 100 µl reservoir solution at either 277 or 291 K. Following the identification of preliminary crystallization leads, crystals were optimized manually using the hanging-drop vapor-diffusion method with 1 µl protein solution plus 1 µl reservoir solution incubated over 1 ml reservoir solution.

Crystal form 1 (*C*222; Fig. 2*a*) was grown by mixing 1.0 µl protein solution (CS buffer plus 0.1% LDAO, with protein at 15 mg ml^{-1}) with an equal volume of reservoir solution containing 50 m*M* Tris–HCl pH 8.5, 13%(*w*/*v*) PEG 1500, 0.03%(*w*/*v*) Anzergent 3-10 and 3%(*w*/*v*) DMSO. Crystals grew to approximately 0.2 × 0.2 × 0.1 mm at 291 K and formed in between 3 and 5 d. Prior to data collection, the crystals were quickly dragged through crystallization solution supplemented with 30%(*w*/*v*) PEG 1500 and 15%(*w*/*v*) glycerol for cryoprotection and were flash-cooled in liquid nitrogen.

Crystal form 2 (*R*32; Fig. 2*b*) and crystal form 3 ($P6_3$; Fig. 2*c*) were grown by mixing 1.0 µl protein solution [CS buffer plus 0.01%(*w*/*v*) TDDG, with protein at 15 mg ml^{-1}] with an equal volume of reservoir solution containing 100 m*M* MES buffer pH 6.0–6.5, 50 m*M* CsCl, 28–32%(*w*/*v*) Jeffamine M-600. The *R*32 crystals preferentially formed from native PorB and grew to maximum dimensions of approximately 0.10 × 0.10 × 0.02 mm in 2–3 weeks at 291 K. Prior to data collection, the crystals were quickly dragged through a crystallization solution with the Jeffamine M-600 concentration increased to 35–40%(*w*/*v*) for cryoprotection, followed by flash-cooling in liquid nitrogen. The $P6_3$ crystal form used the same crystallization conditions as the *R*32 crystal form but preferentially grew from SeMet-incorporated protein. The crystals grew to maximum dimensions of approximately 0.05 × 0.05 × 0.1 mm and formed in 2–3 months.

2.4. Data collection and processing

Crystal quality was assessed by diffraction on Stanford Synchrotron Radiation Laboratory (SSRL) beamlines 9-2 and 11-1, Advanced Light Source (ALS) beamlines 8.2.2 and 8.3.1, Cornell High Energy Synchrotron Source (CHESS) beamlines A1 and F2 and the Advanced Photon Source (APS) Industrial Macromolecular Crystallography Association (IMCA-CAT; ID-17), Southeast Regional Collaborative Access Team (SER-CAT; ID-22) and Life Sciences Collaborative Access Team (LS-CAT; ID-21-D/F/G) beamlines. Iterative rounds of detergent and additive screening improved the diffraction quality of the crystals as assessed by diffraction-based feedback using synchrotron radiation. Even using this procedure, the best crystals of crystal form 1 (*C*222) diffracted to a maximum resolution of 5 Å after careful optimization of the crystallization conditions. As a result, this crystal form was abandoned for structure determination.

Following optimization, crystal form 2 (*R*32) diffracted isotropically to 2.9 Å resolution (Fig. 3*a*) and a complete native data set was collected at 100 K on SSRL beamline 11-1 using a MAR 325 CCD detector. The exposure time was 15 s for each frame and used an oscillation width of 1° per image.

Data for both native and SeMet-incorporated PorB in crystal form 3 ($P6_3$) were collected using a wavelength of 0.978 Å at the APS LS-CAT ID21-G on a MAR 225 CCD detector. A data set consisting of 120 frames was collected with a rotation angle of 90° and an exposure time of 5 s per frame. All data were processed and scaled using the *HKL*-2000 program package (Otwinowski & Minor, 1997).

3. Results and discussion

3.1. Crystallization and data collection

Crystals of the OMP PorB were grown in three different crystal forms (Fig. 2). Initial *C*222 crystals grew from PorB solubilized in

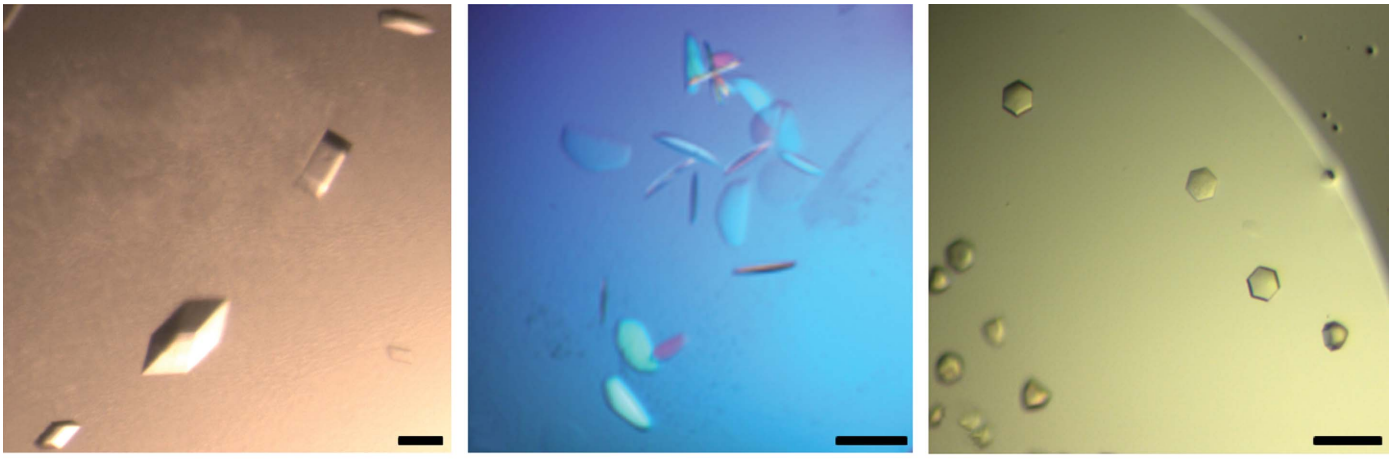

(*a*) (*b*) (*c*)

Figure 2
Crystals of PorB from *N. meningitidis*. Three crystal forms of *N. meningitidis* PorB have been grown using the hanging-drop vapor-diffusion method. (*a*) Crystals of PorB in space group *C*222 were grown using PEG 1500 as a precipitant. (*b*) PorB crystals in space group *R*32 were grown using Jeffamine M-600 as the precipitant. (*c*) SeMet PorB crystals in space group $P6_3$ grown in crystallization conditions identical to those used for the *R*32 space group. The scale bars shown on the figures represent 100 µm.

Table 1
X-ray data-collection statistics.

Values in parentheses are for the highest resolution shell.

Crystal form	*C*222	*R*32	$P6_3$ (SeMet)	$P6_3$ (native)
Wavelength (Å)	1.00	0.979	0.978	0.978
Beamline	SSRL 9-2	SSRL 11-1	SSRL 9-2	APS LS-CAT ID21-G
Resolution (Å)	50–7.0 (7.63–7.0)	50–2.9 (2.97–2.9)	50–2.4 (2.46–2.4)	50–2.3 (2.36–2.3)
Unit-cell parameters (Å, °)	$a = 52.4$, $b = 196.1$, $c = 170.6$, $\alpha = \beta = \gamma = 90$	$a = b = 148.1$, $c = 111.7$, $\alpha = \beta = 90$, $\gamma = 120$	$a = b = 84.7$, $c = 106.1$, $\alpha = \beta = 90$, $\gamma = 120$	$a = b = 83.0$, $c = 106.3$, $\alpha = \beta = 90$, $\gamma = 120$
No. of measured reflections	5663	46100	81980	104141
No. of unique reflections	1156	9700	15842	17123
Multiplicity	4.0 (3.8)	7.5 (5.3)	5.2 (4.0)	6.1 (3.9)
$I/\sigma(I)$	2.6 (1.5)	12.7 (3.4)	19.3 (4.7)	23.1 (3.8)
Completeness (%)	91.4 (91.0)	92.1 (54.8)	94.0 (63.1)	92.0 (61.0)
$R_{\rm merge}$† (%)	11.0 (41.0)	7.5 (12.1)	6.7 (21.5)	6.2 (24.7)
No. of molecules in ASU	1 or 2	1	1	1
Matthews coefficient (Å^3 Da^{-1})	6.1 or 3.0	3.3	2.9	2.9
Solvent content (%)	79 or 59	62	58	58

† $R_{\rm merge} = \sum_{hkl}\sum_i |I_i(hkl) - \langle I(hkl)\rangle| / \sum_{hkl}\sum_i I_i(hkl)$.

0.1% LDAO and used PEG 1000–2000 as the precipitant. These crystals initially diffracted to 20 Å resolution. To optimize diffraction quality, Anzergent and DMSO were included as additives and the precipitant was altered to PEG 1500. However, these alterations only improved the diffraction quality of these crystals to 5 Å resolution.

The *R*32 and $P6_3$ crystals were both grown from TDDG-solubilized PorB with identical crystallization conditions. Both of these crystal forms exhibited reasonable diffraction quality after optimization (Fig. 3, Table 1). Interestingly, PorB crystals in the hexagonal $P6_3$ space group (Fig. 2*c*) were initially identified in crystallization trials of SeMet protein. SeMet PorB only forms crystals in $P6_3$. In comparison, the native protein preferentially crystallizes in the *R*32 space group, but a small percentage (<5%) of native protein formed crystals in space group $P6_3$. Despite growing from identical crystallization conditions, the $P6_3$ crystals exhibited a distinct morphology compared with the *R*32 crystal form (Figs. 2*b* and 2*c*). Data collected at the LS-CAT ID21-G merged to 2.3 Å resolution (Fig. 3*b*; Table 1).

Specific volume calculations (Matthews, 1968) based on the unit-cell parameters and the molecular weight suggested that there could be either one or two PorB molecules per asymmetric unit in the *C*222 crystals, with a Matthews coefficient ($V_{\rm M}$) of 6.1 Å^3 Da^{-1} and a solvent content of 79% for one molecule in the asymmetric unit and a $V_{\rm M}$ of 3.0 Å^3 Da^{-1} and a solvent content of 59% for two molecules in the asymmetric unit. The *R*32 and $P6_3$ crystal forms both contained one molecule in each asymmetric unit. For one molecule in the asymmetric unit, the *R*32 crystals have a $V_{\rm M}$ value of 3.3 Å^3 Da^{-1} and a solvent content of 62%, while the $P6_3$ crystal form has a $V_{\rm M}$ of 2.9 Å^3 Da^{-1} and a solvent content of 58%.

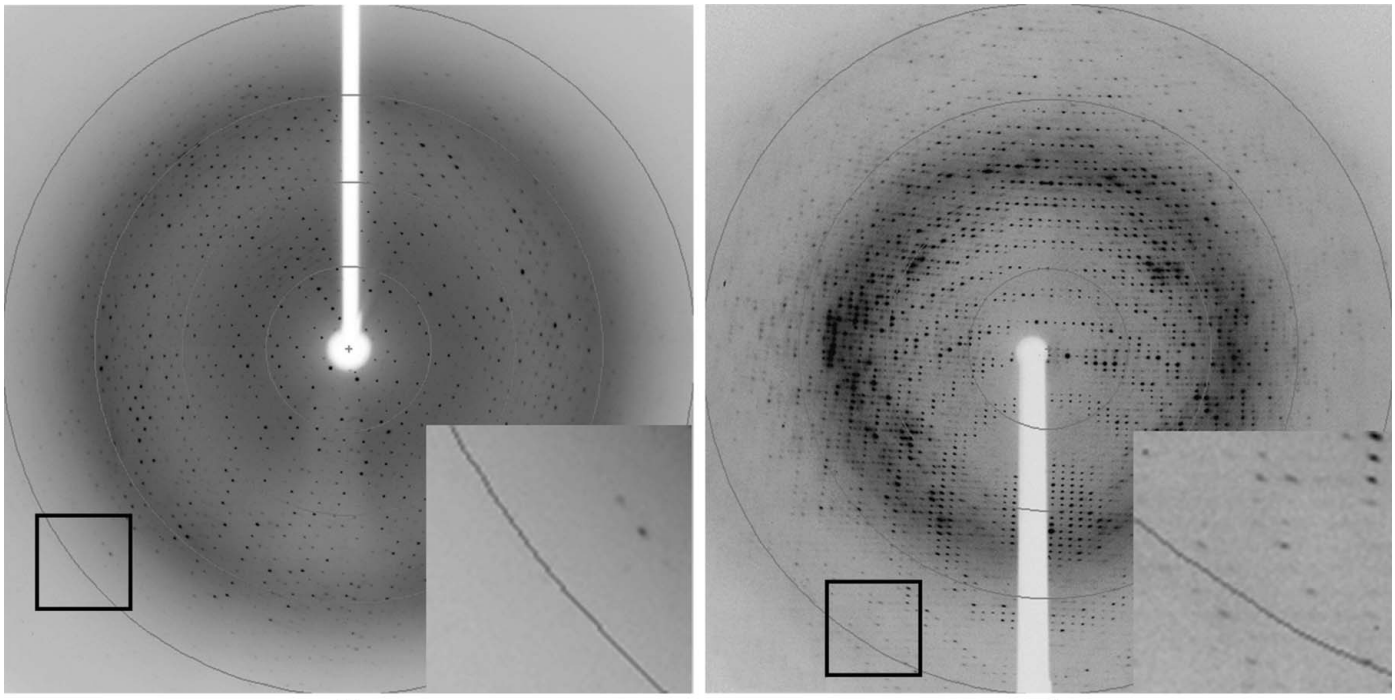

(*a*) (*b*)

Figure 3
Typical X-ray diffraction patterns of the *R*32 and $P6_3$ crystal forms. (*a*) Diffraction image from the *R*32 crystal form collected on SSRL beamline 11-1. The oscillation angle was 1°. Circles superimposed onto the diffraction pattern correspond to resolutions of 10.8, 5.4, 3.6 and 2.7 Å. In the magnified inset, diffraction spots extending to 2.8 Å resolution can be observed. (*b*) Diffraction image from the $P6_3$ crystal form collected at the APS LS-CAT ID21-G. The oscillation angle was 0.75°. Circles superimposed onto the diffraction pattern correspond to resolutions of 8.5, 4.3, 2.8 and 2.1 Å. In the magnified inset, diffraction spots extending to 2.0 Å resolution can be observed.

Table 2
X-ray data-collection statistics for PorB heavy-atom derivative crystals.

Values in parentheses are for the highest resolution shell.

	SeMet crystal soaked with		
	Lutetium acetate	Sodium tungstate	Erbium acetate
Wavelength (Å)	1.314	0.978	1.29
Beamline	ALS 8.3.1	ALS 8.3.1	CHESS F2
Resolution (Å)	50–3.5 (3.59–3.5)	50–2.7 (2.77–2.7)	50–3.3 (3.38–3.3)
Unit-cell parameters (Å, °)	$a = b = 83.6$, $c = 106.1$, $\alpha = \beta = 90$, $\gamma = 120$	$a = b = 84.6$, $c = 105.8$, $\alpha = \beta = 90$, $\gamma = 120$	$a = b = 84.4$, $c = 106.6$, $\alpha = \beta = 90$, $\gamma = 120$
No. of measured reflections	41921	88230	40382
No. of unique reflections	5358	11050	6562
Multiplicity	7.8 (7.6)	8.0 (6.2)	6.2 (6.1)
$I/\sigma(I)$	14.5 (5.8)	18.5 (3.3)	11.5 (3.8)
Completeness (%)	98.8 (98.2)	93.0 (60.2)	99.9 (100)
$R_{\rm merge}$† (%)	11.8 (44.3)	8.8 (31.0)	11.3 (45.8)

† $R_{\rm merge} = \sum_{hkl}\sum_i |I_i(hkl) - \langle I(hkl)\rangle| / \sum_{hkl}\sum_i I_i(hkl)$.

3.2. Identification of heavy-atom derivatives

N. meningitidis PorB contains only two methionine residues and does not have significant sequence similarity to any porin of known structure. As a result, phasing of the *N. meningitidis* PorB primarily used the method of multiple isomorphous replacement with anomalous scattering after heavy-atom incorporation. Since the SeMet PorB had a dramatically increased likelihood of forming in the $P6_3$ crystal form, which had the highest diffraction limit, heavy-atom cocrystallizations and soaks were performed on SeMet protein. Three derivatives, Lu^{3+}, Er^{3+} and WO_4^{2-}, were prepared by soaking SeMet PorB crystals with 1 m*M* lutetium acetate for 3 h, 1 m*M* sodium tungstate for 3 h or 5 m*M* erbium acetate for 3 d. Data were collected using the wavelengths and beamlines listed in Table 2. The location of the position of Lu^{3+} was identified using the *SHELXD* (Sheldrick, 2008) subroutine in the program *SHARP* (de La Fortelle & Bricogne, 1997). Sites for the other two heavy atoms and the SeMet locations were identified using difference Fourier maps phased with the Lu^{3+} derivative. The details of the structure determination and analysis will be published elsewhere.

This work was supported by a grant from the Ellison Medication Foundation (AG-NS-0325) and NIH grants GM081816 and GM079419. MT was supported by The Uehara Memorial Foundation. Portions of this research were carried out at beamlines 9-2 and 11-1 at Stanford Synchrotron Radiation Light Source (SSRL), a national user facility operated by Stanford University on behalf of the US Department of Energy, Office of Basic Energy Sciences. The SSRL Structural Molecular Biology Program is supported by the Department of Energy, Office of Biological and Environmental Research and by the National Institutes of Health, National Center for Research Resources, Biomedical Technology Program and the National Institute of General Medical Sciences. Use of Industrial Macromolecular Crystallography Association (IMCA-CAT) ID-17, Southeast Regional Collaborative Access Team (SER-CAT) ID-22 and the Life Sciences Collaborative Access Team (LS-CAT) ID21-G beamlines at Advanced Photon Source (APS) was supported by the US Department of Energy, Office of Science, Office of Basic Energy Sciences under Contract No. DE-AC02-06CH11357. Beamline 8.3.1 at Advanced Light Source (ALS) is supported by the Director, Office of Science, Office of Basic Energy Sciences of the US Department of Energy under Contract No. DE-AC02-05CH11231. The Cornell High Energy Synchrotron Source (CHESS) A1 and F2 stations are supported by the NSF and NIH/NIGMS *via* NSF award DMR-0225180 and the MacCHESS resource is supported by NIH/NCRR award RR-01646. We thank Dr YiWei Tang for the clinical isolate of *N. meningitidis*, Dr David Friedman for mass-spectroscopic analysis, Dr Jessica Vey, Timothy Panosian, and Thomas Tomasiak for experimental assistance with the data collection and Dr Jessica Vey, Timothy Panosian and Tarjani Thaker for critical reading of the manuscript.

References

Derrick, J. P., Urwin, R., Suker, J., Feavers, I. M. & Maiden, M. C. (1999). *Infect. Immun.* **67**, 2406–2413.
Feavers, I. M., Suker, J., McKenna, A. J., Heath, A. B. & Maiden, M. C. (1992). *Infect. Immun.* **60**, 3620–3629.
Girard, M. P., Preziosi, M. P., Aguado, M. T. & Kieny, M. P. (2006). *Vaccine*, **24**, 4692–4700.
Kilic, A., Urwin, R., Saracli, M. A., Stratton, C. W. & Tang, Y. W. (2006). *J. Clin. Microbiol.* **44**, 222–224.
La Fortelle, E. de & Bricogne, G. (1997). *Methods Enzymol.* **276**, 472–494.
Ley, P. van der, Heckels, J. E., Virji, M., Hoogerhout, P. & Poolman, J. T. (1991). *Infect. Immun.* **59**, 2963–2971.
Locher, K. P. & Rosenbusch, J. P. (1997). *Eur. J. Biochem.* **247**, 770–775.
Massari, P., Ho, Y. & Wetzler, L. M. (2000). *Proc. Natl Acad. Sci. USA*, **97**, 9070–9075.
Massari, P., Ram, S., Macleod, H. & Wetzler, L. M. (2003). *Trends Microbiol.* **11**, 87–93.
Massari, P., Visintin, A., Gunawardana, J., Halmen, K. A., King, C. A., Golenbock, D. T. & Wetzler, L. M. (2006). *J. Immunol.* **176**, 2373–2380.
Matthews, B. W. (1968). *J. Mol. Biol.* **33**, 491–497.
Minetti, C. A., Tai, J. Y., Blake, M. S., Pullen, J. K., Liang, S. M. & Remeta, D. P. (1997). *J. Biol. Chem.* **272**, 10710–10720.
Moeck, G. S. & Coulton, J. W. (1998). *Mol. Microbiol.* **28**, 675–681.
Müller, A., Günther, D., Düx, F., Naumann, M., Meyer, T. F. & Rudel, T. (1999). *EMBO J.* **18**, 339–352.
Müller, A., Rassow, J., Grimm, J., Machuy, N., Meyer, T. F. & Rudel, T. (2002). *EMBO J.* **21**, 1916–1929.
Nøkleby, H., Aavitsland, P., O'Hallahan, J., Feiring, B., Tilman, S. & Oster, P. (2007). *Vaccine*, **25**, 3080–3084.
Otwinowski, Z. & Minor, W. (1997). *Methods Enzymol.* **276**, 307–326.
Qi, H. L., Tai, J. Y. & Blake, M. S. (1994). *Infect. Immun.* **62**, 2432–2439.
Rudel, T., Schmid, A., Benz, R., Kolb, H. A., Lang, F. & Meyer, T. F. (1996). *Cell*, **85**, 391–402.
Sheldrick, G. M. (2008). *Acta Cryst.* A**64**, 112–122.
Singleton, T. E., Massari, P. & Wetzler, L. M. (2005). *J. Immunol.* **174**, 3545–3550.
Stephens, D. S., Greenwood, B. & Brandtzaeg, P. (2007). *Lancet*, **369**, 2196–2210.
Tanabe, M. & Iverson, M. T. (2009). *Curr. Top. Membr.* **63**, 229–267.
Van Duyne, G. D., Standaert, R. F., Karplus, P. A., Schreiber, S. L. & Clardy, J. (1993). *J. Mol. Biol.* **229**, 105–124.
Wiener, M. C. (2005). *Curr. Opin. Struct. Biol.* **15**, 394–400.
Wright, J. C., Williams, J. N., Christodoulides, M. & Heckels, J. E. (2002). *Infect. Immun.* **70**, 4028–4034.